

# RETRACTED ARTICLE: Fabrication and characterization of glimepiride nanosuspension by ultrasonication-assisted precipitation for improvement of oral bioavailability and in vitro $\alpha$ -glucosidase inhibition

This article was published in the following Dove Press journal:  
International Journal of Nanomedicine

Haroon Rahim<sup>1</sup>  
Abdul Sadiq<sup>2</sup>  
Shahzeb Khan<sup>2-4</sup>  
Fazli Amin<sup>1</sup>  
Riaz Ullah<sup>5</sup>  
Abdelaaty A Shahat<sup>5,6</sup>  
Hafiz Majid Mahmood<sup>7</sup>

<sup>1</sup>Department of Pharmacy, Sarhad University of Science and Information Technology, Peshawar, Khyber Pakhtunkhwa, 25000, Pakistan;

<sup>2</sup>Department of Pharmacy, University of Malakand, Chakdara, Khyber Pakhtunkhwa, 18800, Pakistan;

<sup>3</sup>Discipline of Pharmaceutical Sciences, School of Health Sciences, University of KwaZulu-Natal, Durban, 4000, South Africa;

<sup>4</sup>Division of Molecular Pharmaceutics and Drug Delivery, College of Pharmacy, The University of Texas at Austin, Austin, TX, USA;

<sup>5</sup>Department of Pharmacognosy (MAPPRC), College of Pharmacy, King Saud University, Riyadh, Saudi Arabia;

<sup>6</sup>Phytochemistry Department, National Research Centre, Giza, Egypt;

<sup>7</sup>Department of Pharmacy, College of Pharmacy, King Saud University, Riyadh 11451, Saudi Arabia

**Purpose:** We aimed to enhance the solubility, dissolution rate, oral bioavailability, and  $\alpha$ -glucosidase inhibition of glimepiride (Glm) by fabricating its nanosuspension using a precipitation-ultrasonication approach.

**Methods:** Glm nanosuspensions were fabricated using optimized processing conditions. Characterization of Glm was performed using Malvern Zetasizer, scanning electron microscopy, transmission electron microscopy, differential scanning calorimetry, and powder X-ray diffraction. Minimum particle size and polydispersity index (PDI) values were found to be  $152.4 \pm 2.42$  nm and  $0.23 \pm 0.01$ , respectively, using hydroxypropyl methylcellulose: 6 cPs, 1% w/v, polyvinylpyrrolidone K30 1% w/v, and sodium lauryl sulfate 0.12% w/v, keeping ultrasonication power input at 99 W, with 15 minutes' processing at 3-second pauses. In vivo oral bioavailability was assessed using rabbits as a model.

**Results:** The saturation solubility of the Glm nanosuspensions was substantially enhanced 3.14-fold and 5.72-fold compared to unprocessed drug in stabilizer solution and unprocessed active pharmaceutical ingredient. Also, the dissolution rate of the nanosuspensions was substantially boosted when compared to the marketed formulation and unprocessed drug candidate. The results showed that 35% of Glm nanosuspensions dissolved in the first 10 minutes compared to 10.17% of unprocessed Glm, 42.19% of microsuspensions, and 19.94% of marketed tablets. In-vivo studies conducted in animals, i.e. rabbits, demonstrated that maximum concentration and  $AUC_{0-24}$  with oral dosing were twofold (5 mg/kg) and 1.74-fold (2.5 mg/kg) and 1.80-fold (5 mg/kg) and 1.63-fold (2.5 mg/kg), respectively, and compared with the unprocessed drug formulation. In-vitro  $\alpha$ -glucosidase inhibition results showed that fabricated nanosuspensions had a pronounced effect compared to unprocessed drug.

**Conclusion:** The optimized batch fabricated by ultrasonication-assisted precipitation can be useful in boosting oral bioavailability, which may be accredited to enhanced solubility and dissolution rate of Glm, ultimately resulting in its faster rate of absorption due to nanonization.

**Keywords:** glimepiride nanosuspension, precipitation-ultrasonication approach, boosted bioavailability

Correspondence: Haroon Rahim  
Department of Pharmacy, Sarhad University of Science and Information Technology Peshawar, Peshawar 2500, Khyber Pakhtunkhwa, Pakistan  
Tel +92 332 946 1642  
Email hrahimpk@gmail.com

## Introduction

It has been observed that many active pharmaceutical ingredients (APIs) display low aqueous solubility and bioavailability during the drug-development stage.<sup>1</sup> Recently, nanosuspension has been successfully fabricated to overcome

this challenge in either a top-down or bottom-up fashion.<sup>2,3</sup> The last decade witnessed the bottom-up approach being used to accomplish APIs in the nano-sized range.<sup>4,5</sup> To prepare nanosized or micronized drug particles, antisolvent precipitation is considered an effective method. One antisolvent-precipitation approach involves dissolution of the drug candidate in the solvent phase, followed by it being introduced into an antisolvent phase, ultimately leading to the drug's precipitation. This approach is an effective and commonly employed bottom-up approach for fabricating nanosuspension, owing to simplicity and low cost.<sup>6,7</sup> However, the approach still faces issues of maintaining accurate particle size, obtaining stability after precipitation, and scaling up of batches.<sup>6,8–10</sup> Ultrasonication combined with precipitation is an effective approach to attain improved particle-size reduction. This process is responsible for controlling the two processes of nucleation and crystallization. When applied on fluid, ultrasonic notes are characterized by two phases:

- expansion: a cyclic series that exerts negative pressure
- compression: positive pressure holding molecules together

By initiating cavitation bubbles, ultrasound notes also intensify mass transfer, which is formed during the expansion phase. A large magnitude of energy is released due to the formation, growth, and consequent collapse of bubbles. Powerful shock waves are released once a bubble collapses, then a confined hot spot with high temperature and pressure is formed. Consequently, mixing of the two phases (solvent and antisolvent) is boosted, leading to “supersaturation” of the mixture. Moreover, the collapse of vacuum bubble causes the breakdown of the particles. The process depends on the duration and intensity of

sonication energy, horn length and depth of immersion, and temperature.<sup>11–14</sup>

Soluble polymers, such as cellulosic polymers, hydroxypropyl methylcellulose (HPMC), polyvinylpyrrolidone (PVP), and polyvinyl alcohol, are among the common polymers/stabilizers used to achieve stability.<sup>15</sup> These stabilizers are used at 1%–7.5% w:v in nanosuspension formulations.<sup>16,17</sup> Glimepiride (Glm) is an oral sulfonylurea derivative, as shown in Figure 1. It has been used in the treatment of type 2 diabetes mellitus for many years. It is practically insoluble in water and is a biopharmaceutical classification–system class 2 drug.<sup>18,19</sup> As such, it will be essential to produce a stable Glm nanosuspension (GN) to enhance low water solubility and ultimately boost bioavailability. In this study, stabilized GNs were fabricated using ultrasonication-assisted precipitation with the aim of increasing solubility, in vitro dissolution, and ultimately oral bioavailability of Glm.

## Methods

### Materials

Glm (batch 004092013) and (sodium lauryl sulfate (SLS) were a generous gift from Bryon Pharmaceuticals, Peshawar, Pakistan. HPMC grade 6 cPs, PVP K30, acetone, and methanol were purchased from a market in Peshawar, Khyber Pakhtunkhwa, Pakistan. All experimental studies on animals were conducted as per protocols (Pharm/AEC/G-04–07) approved by the Animal Ethical Committee, University of Malakand, Khyber Pakhtunkhwa, Pakistan and relevant bye-laws (2008).

### Fabrication of glimepiride nanosuspension

GN was fabricated using a precipitation–ultrasonication method. In brief, 50 mg Glm solutions were fabricated in acetone and methanol 6 mL (1:1) as organic solvents, added dropwise to the antisolvent phase, precooled at 4°C,

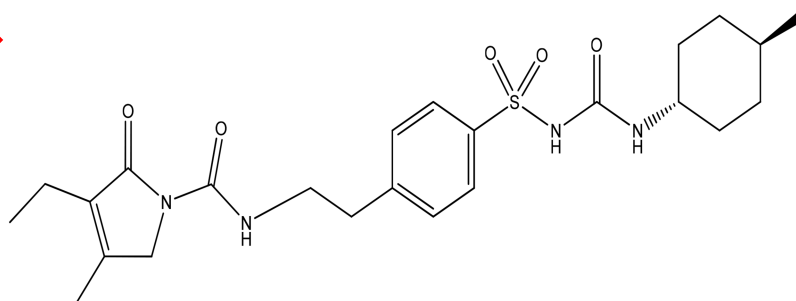


**Figure 1** Chemical structure of glimepiride.

containing different concentrations of polymers ie PVP K30, HPMC grade 6 cPs, and SLS at 1,500 rpm using a magnetic stirrer. Later, ultrasonication was carried out for the fabricated suspension at different intervals (10–30 minutes) at different ultrasonic energy input, i.e. 100, 200, 300, 400, and 500 W, at 3-second pauses. The initial particle size of the suspension was measured using a Malvern Zetasizer.<sup>20</sup> Subsequently, after optimizing the processing parameters and conditions for preparation of GN, the size of the batch was successfully scaled up from 5 mL to 400 mL.

## Drying of glimepiride nanosuspensions

The milky GN prepared earlier was centrifuged at 5,000 rpm for 10 minutes. Then, the supernatant was discarded and sedimented particles oven-dried for 60 minutes and stored in borosilicate glass vials at room temperature for further analysis in a desiccator.

## Characterization of glimepiride nanosuspension

### Particle-size analysis and $\zeta$ -potential measurement

The Zetasizer was used for evaluation of  $\zeta$ -potential and particle size of GNs. GNs were diluted with water for size measurement.<sup>21</sup>

### Content analysis of glimepiride

Mohd et al<sup>22</sup> method was used. An HPLC system with an ultraviolet-visible detector was used. Conditions were acetonitrile: 0.2 M phosphate buffer (pH 7.4) as the mobile phase, Hypersil BDS C<sub>18</sub> (250×4.6 mm) column, 5  $\mu$ m, and at 1 mL/min flow rate, injection volume 20  $\mu$ L at 25°C temperature with 25 minute run time, and 228 nm detection wavelength.

## Scanning electron microscopy

Unprocessed Glm was subjected to scanning electron microscopy (Quanta 400) for morphological analysis. Glm images were observed at suitable magnification powers.<sup>23</sup>

## Transmission electron microscopy

Transmission electron microscopy (TEM; TEM 1200) was used for evaluation of Glm. Nanosuspensions were dropped on copper–gold carbon grids and dried at room temperature, followed by taking photographing at suitable magnification.<sup>24</sup>

## X-ray diffraction

X-ray diffraction (XRD) studies of unprocessed drug, physical mixture, and GN were carried out using PANalytical X'pert powder.<sup>24</sup>

## Differential scanning calorimetry

Thermal properties of both unprocessed and GN were recorded using differential scanning calorimetry (DSC) (Shimadzu TA60). In aluminum pans, 5 mg samples were heated at a scanning rate of 10°C/min at 40°C–200°C under a nitrogen flow of 50 mL/min.<sup>25</sup>

## Saturation solubility

GNs (1.5 mL) were put into centrifugation tubes and centrifuged at 14,800 rpm for 30 minutes. Then, of Glm concentrations in the supernatant already filtered through 0.2  $\mu$ m filters were determined using HPLC. Likewise, the saturation solubility of Glm in the stabilizer (w/v) solution (ie, HPMC, PVP K30, SLS) and aqueous medium was assessed to find out the impact of nanoparticles on drug (Glm) solubility. All samples were evaluated in triplicate.<sup>24</sup>

## Stability

Stability studies were conducted to evaluate particle growth caused by aggregation and Ostwald ripening. Physical stability of GNs was assessed by keeping them stable for 90 days at 2°C–8°C, 25°C, and 40°C, while chemical stability of was evaluated by active pharmaceutical contents of the stored samples for 3 months using the method mentioned earlier. At different time intervals (10, 15, 30, 45, 60, 75, and 90 days), particle size and PDI values were recorded using the Zetasizer.<sup>23</sup>

## In vitro dissolution

The dissolution (in-vitro) was conducted in dissolution medium, i.e., PBS (900 mL, pH 7.4) for Glm, GN, and a marketed product, ie, tablets. GN was prepared by dispersing crushed tablets of Glm in stabilizer solution (HPMC 0.5 w/v) in medium, as used for the raw drug, nanoformulation, and tablets, keeping the temperature at 37°C±0.5°C with paddles operating at 100 rpm. Sample aliquots (5 mL) were collected and filtered via 0.4  $\mu$ m membrane filter at 0, 5, 10, 15, 30, 45, and 60 minutes. Each time, fresh medium (5 mL) was added to the dissolution medium. The amount of drug was determined by HPLC.<sup>22</sup>

## In vivo bioavailability

In sum, 24 rabbits weighing 2.5–3.0 kg were divided into four groups (six per group) and housed in cages with free access to water and food. Glm was given in doses of 5 and 2.5 mg/kg, and the fabricated optimized GN given orally at doses of 5 and 2.5 mg/kg. Blood was collected in heparinized tubes at 0, 0.5, 1, 1.5, 2, 4, 6, 8, 12, and 24 hours, after dosing. Plasma was separated from blood immediately by centrifugation at 3,000 rpm for 20 min and frozen until analysis using the HPLC method of Mohd et al. All animal experiments were carried out in accordance with the approved protocols mentioned earlier.<sup>22,26</sup> The main pharmacokinetic parameters were acquired with the help of PK Solutions 2.0 noncompartmental pharmacokinetic data-analysis software. Statistical analysis was done using ANOVA followed by Tukey's post hoc testing to determine the significance of any differences.

## In vitro $\alpha$ -glucosidase inhibition

$\alpha$ -Glucosidase inhibition was assessed as per Artanti et al.<sup>27</sup> Samples (amount 0.1 mL) were added to test tube containing 0.1 mL 20 mM pNPG (*p*-nitrophenyl  $\alpha$ -D-glucopyranoside) and 100 mM PBS (2.2 mL) at pH 7 followed by incubating it at 37°C for 5 minutes. The reaction was initiated by addition of 0.1 mL enzyme solution (1 mg/0.1 mL), followed 15 minutes' incubation at 37°C. The reaction was stopped by addition of 200 mM Na<sub>2</sub>CO<sub>3</sub> (2.5 mL). Absorbance of *p*-nitrophenol released from *p*-nitrophenyl  $\alpha$ -glucopyranoside, was measured spectrophotometrically at 400 nm. Inhibition of  $\alpha$ -glucosidase was calculated:

$$[1 - (A/P)] \times 100\%$$

where B represent absorbance in absence of the sample and A absorbance in presence of the sample.

## Results and discussion

### Optimum processing parameters for preparation of glimepiride nanosuspension

Initially, a concentration (w/v) of 0.5% of each of HPMC and PVP K30 was used while keeping 0.12% SLS to fabricate suspension. The optimized GN was stabilized by 1% HPMC, 1% PVP K30, and 0.12% SLS, as represented in Figure 2. Further increasing the concentration of stabilizers enhanced particle size. Furthermore, particle size increased with further increasing the concentration of polymer used, e.g. PVP K30

which might have been due to the higher viscosity of the resulting solution.<sup>29</sup> TEM clearly displayed even particle-size distribution <200 nm (Figure 4B). A noticeable reduction was observed in the final particle size (152.4±2.42 nm) of fabricated GN from 15–25  $\mu$ m and 110–120  $\mu$ m, as revealed in Figure 4A. The impact of ultrasonication power on particle size was evaluated. Duration was kept at 15 minutes and ultrasonication at 400 W, respectively, as depicted in Figure 3A and B. The duration of sonication had a vital effect on particle size when power was fixed at 400 W. 5 minutes' sonication being too short to fabricate a nanosuspension of desired particle size. Sonication temperature similarly affected particle size. Commonly, a lower temperatures smaller crystals are formed. High temperatures enhances drug solubility, with subsequent reduction in supersaturation and numbers of nuclei. The temperature effect may be explained by relating to a higher rate of diffusion and kinetic reaction at crystal surfaces, ultimately resulting in improved crystal growth.<sup>30</sup>

Boosted erosion on large crystal surfaces and agglomeration resulted from this precipitation-assisted ultrasonication. These results can be easily explained. First, a higher precipitation temperature improved the saturation solubility of Glm in the solution and thereafter decreased supersaturation, which resulted in a lower nucleation rate and consequently larger crystals. Secondly, once nucleation had been achieved, crystal growth was believed to occur in the following steps:

Step I: diffusion of drug molecules from bulk solution to solid crystal interface

Step II: assimilation of drug molecules into crystal lattice with release of heat of crystallization

Step III: conductance of heat of crystallization into bulk solution

At higher temperatures, faster crystal growth occurred, owing to higher diffusion and improved reaction kinetics at the crystal interface. Moreover, the extent of Ostwald ripening was reduced, owing to reduction in saturation solubility with falling temperature, leading to smaller PDI values.<sup>31</sup>

## DSC

Unprocessed Glm exhibited an endothermic peak at 212°C, conforming to its melting point, as the thermogram depicts in Figure 5.<sup>32</sup> GN (optimized nanoformulation) exhibited a

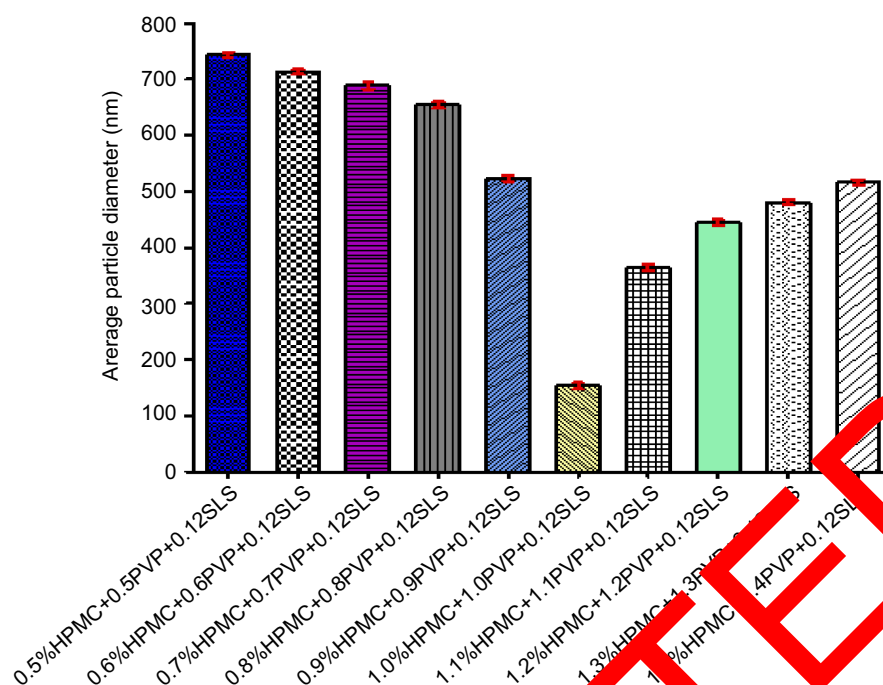


**Figure 2** Influence of polymer concentration on particle size.

**Abbreviations:** HPMC, hydroxypropyl methylcellulose; PVP, polyvinylpyrrolidone; SLS, sodium lauryl sulfate.

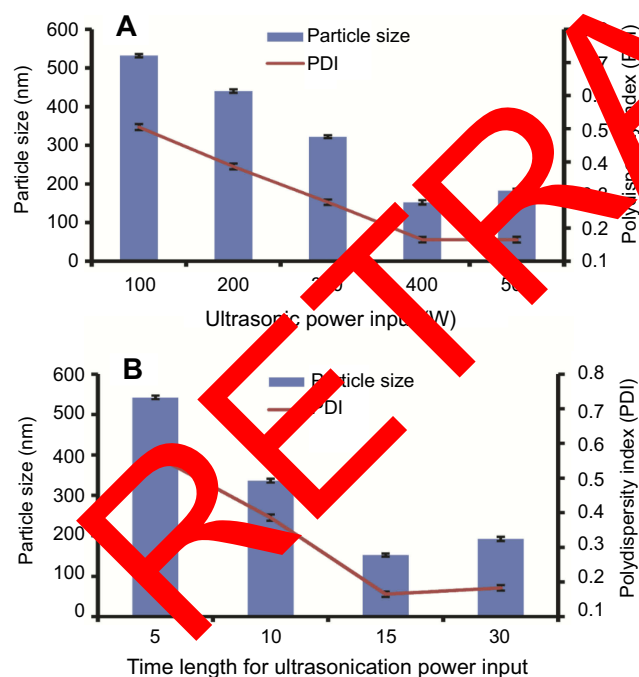


**Figure 3** Impact of ultrasonic energy power input (A) and time length (B) on particle size of fabricated GN.

**Abbreviation:** GN, glimepiride nanosuspension.

minor shift in melting point at 205°C. Alterations in melting points might have been due to particle-size variance between the unprocessed API and fabricated optimized GN. The DSC

peak broadening result may have been due to the presence of traces of polymeric materials on the surfaces of drug particles.<sup>33,34</sup>

## Powder XRD

Powder-XRD patterns displayed that processed Glm was of crystalline nature (Figure 6). However, peak intensities of nanoparticles were comparatively low in comparison to unprocessed Glm. This outcome was due to the nanonizing process.

Moreover, smaller particles and the presence of trace amorphous polymeric materials caused decreases in GN peaks (Figure 6).<sup>21,35,36</sup> Additionally, the powder-XRD pattern of the physical mixture exhibited dominant peaks for Glm particles, whereas peaks for small amounts of polymeric materials (amorphous nature) disappeared.

## Saturation solubility

The low solubility of Glm in aqueous medium was boosted significantly ( $P<0.05$ ) by reducing its particle size. The solubility ( $\mu\text{g/mL}$ ) of the unprocessed drug (Glm) in water was  $25.83\pm4.79$ , GN in water  $149.0\pm5.96$ , and unprocessed Glm in stabilizer solution  $43.81\pm4.75$ , while GN exhibited almost 5.97-fold improved saturation solubility in comparison to the unprocessed



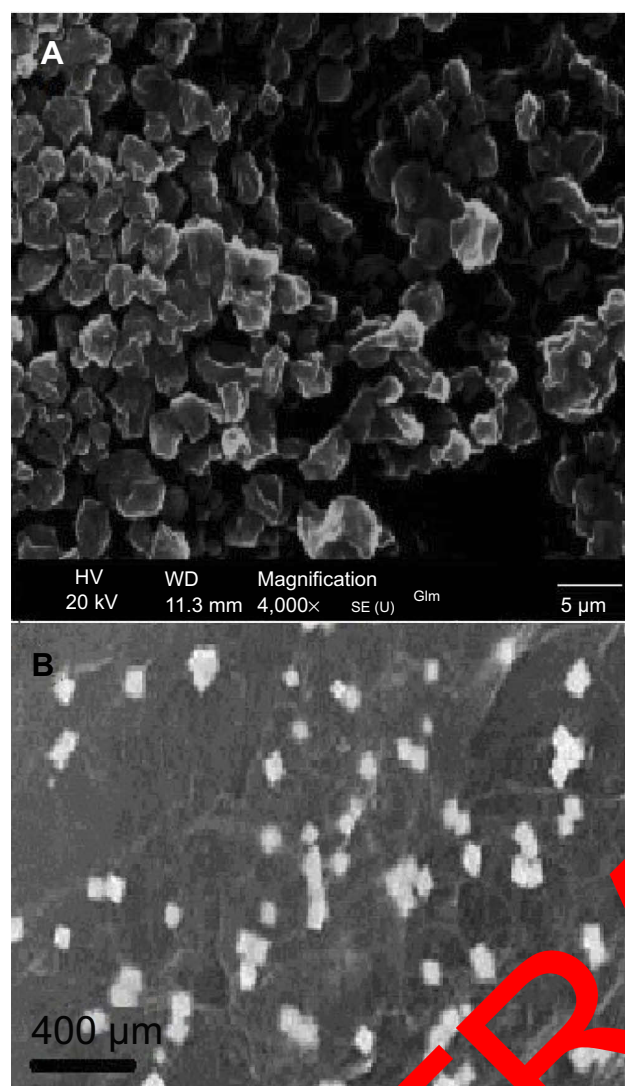


**Figure 4** SEM of raw glimepiride (Glm) (A); TEM of Glm nanosuspension (B).  
**Abbreviations:** SEM, scanning electron microscopy; TEM, transmission electron microscopy; HV, high vacuum; WD, working distance.

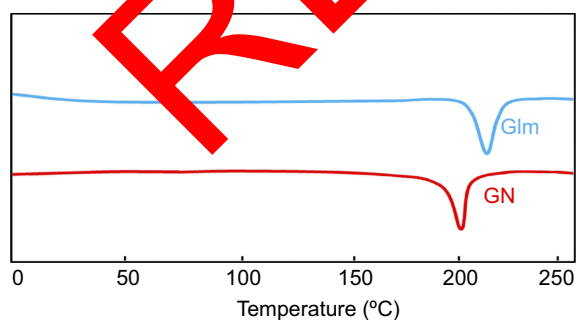


**Figure 5** DSC thermogram of GN and unprocessed Glm.  
**Abbreviations:** DSC, differential scanning calorimetry; Glm, glimepiride; GN, Glm nanosuspension.

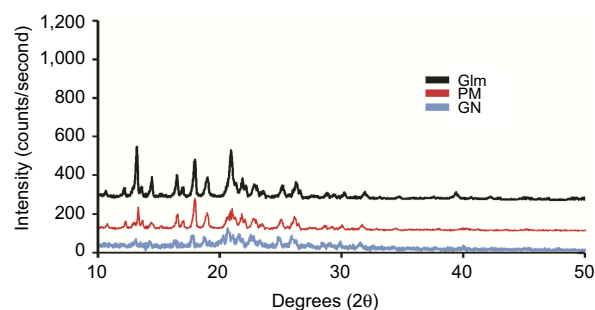


**Figure 6** P-XRD patterns of GN, unprocessed Glm, and PM.  
**Abbreviations:** P-CRD, powder X-ray diffraction; Glm, glimepiride (unprocessed); GN, Glm nanosuspension; PM, physical mixture.

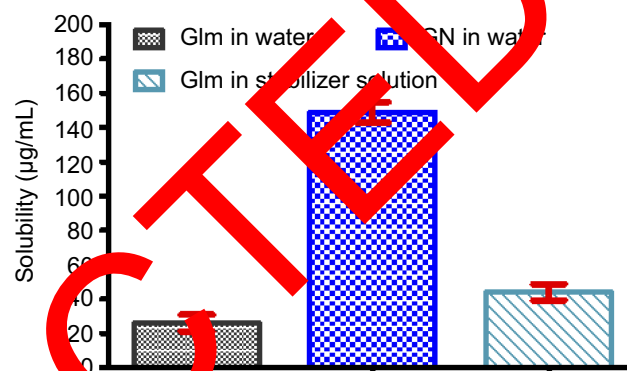


**Figure 7** Solubility of Glm, GN in aqueous medium, and Glm in stabilizer solution.  
**Abbreviations:** Glm, glimepiride; GN, glimepiride nanosuspension.

Glm and 3.50-fold boosted in comparison to Glm in the stabilizer solution as depicted in Figure 7.

## Stability

The physical stability of GN stored at 2°C–8°C and 25°C (Figure 8, A and B) showed maximum stability with preserved PDI values when compared with the samples stored at 40°C (Figure 8C). At high temperatures, interparticle interaction of suspended particles increased, owing to an increase in kinetic energy.<sup>37</sup> Freitas and Müller suggested that to attain a stabilized nanosuspension formulation, 2°C–8°C is favorable.<sup>38</sup>

The ζ-potential values were  $-24.1 \pm 1.2$  mV and  $-28.02 \pm 1.09$  mV for the batch size of 100 and 300 mL respectively, as displayed in below Figure 9.

The value of ζ-potentials is a judgment of the electrical charge at the surface of particles that ensures the physical stability of fabricated nanosuspensions. This has been reported as  $\pm 30$  mV for an electrostatically stabilized nanoformulation and  $\pm 20$  mV for a sterically stabilized one.<sup>39,40</sup> The active contents of GN were  $98.05\% \pm 2.50\%$ , which proved the efficient use of technology and stability of GN using the combinative technique (Table 1).

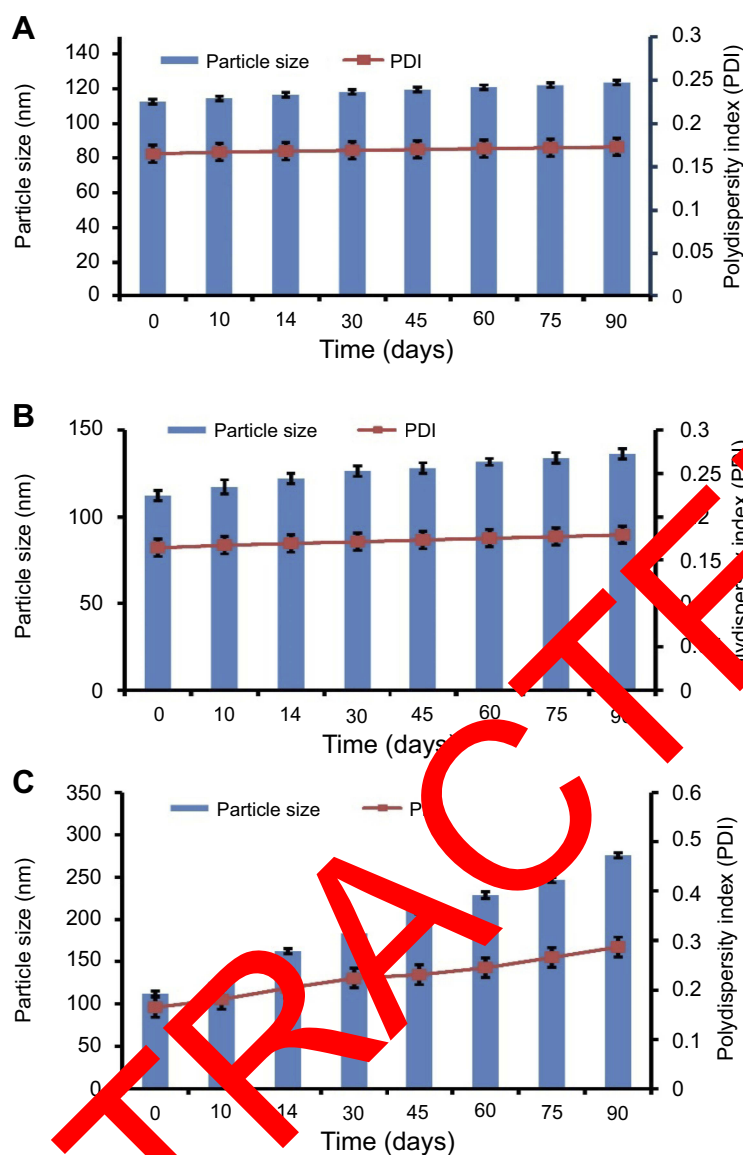


**Figure 8** Physical stability of GN in terms of P.S and PDI at (A) 2°C–8°C, (B) 25°C, and (C) 40°C.  
**Abbreviations:** GN, glimepiride nanosuspension; PDI, polydispersity index.

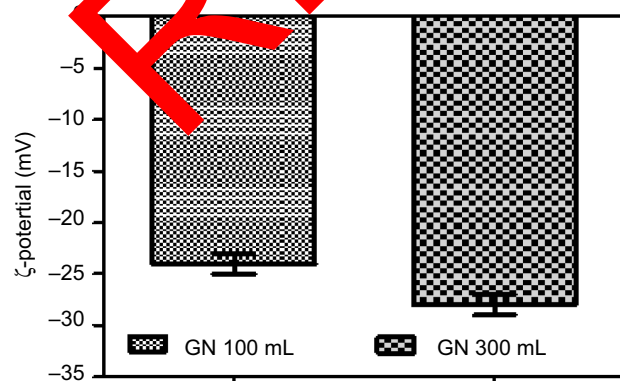


**Figure 9**  $\zeta$ -potential of glimepiride nanosuspension (GN).

**Table I** Chemical stability of glimepiride nanosuspension

Day	Active content (%)	Day	Active content (%)
0	99.25±1.55	45	95.88±1.22
10	98.31±1.08	60	94.14±1.42
15	97.94±1.15	75	93.66±1.06
30	96.76±1.04	90	92.62±1.18

**Note:** Values expressed as means  $\pm$  SD.

### In vitro dissolution

Dissolution profiles of raw Glm, GN, and an available marketed formulation, i.e. tablets, are presented in Figure 10. A significantly enhanced dissolution rate for fabricated GN was

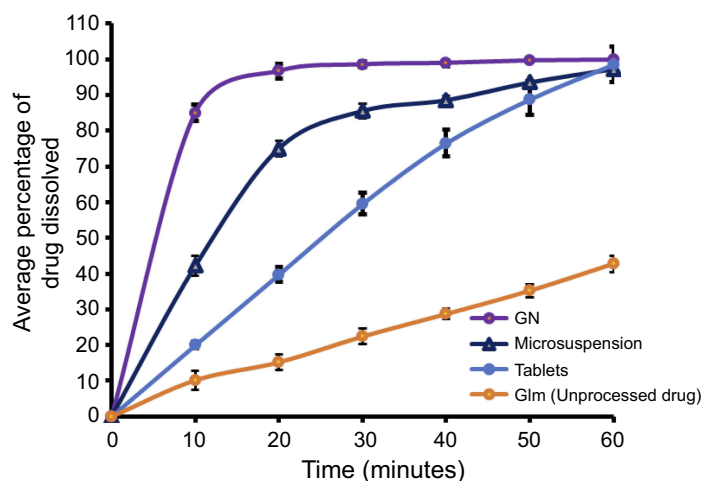


**Figure 10** Comparative in vitro dissolution profiles of raw glimepiride (Glm), Glm nano suspension (GN), and marketed tablets.

shown in comparison to unprocessed Glm and the marketed tablets. In the first 10 minutes, >85% of GN was dissolved compared to 10.17% of unprocessed Glm, 42.19% of micro-suspension, and 20.44% of the marketed tablets. When particles are reduced to nanosize, the solubility of the drug candidate will be improved, as described by Xia et al, who explained the connection between particle size and drug solubility.<sup>41</sup>

### In vivo bioavailability

GN exhibited boosted absorption in comparison to unprocessed Glm. At 5 mg/kg oral dose, there was a doubling of  $C_{max}$  and 1.8-fold enhancement in  $AUC_{0-24}$  of GN-I in

comparison to the unprocessed API. Also, GN-II at a dose of 2.5 mg/kg orally resulted in 1.74-fold enhanced  $C_{max}$  and 1.63-fold boosted  $AUC_{0-24}$  when compared to the unprocessed API. The results verified a marked improvement in  $C_{max}$  of Glm after oral administration of API at different doses as depicted in Figure 11 and Table 2.

### In vitro $\alpha$ -glucosidase inhibition

The  $\alpha$ -glucosidase inhibition-assay results showed that the fabricated GN had marked potential compared to unprocessed Glm (Table 3). GN showed markedly enhanced  $\alpha$ -glucosidase inhibition ( $IC_{50}=21.30 \mu\text{g/mL}$ ) compared to Glm ( $IC_{50} = 49.52 \mu\text{g/mL}$ ).

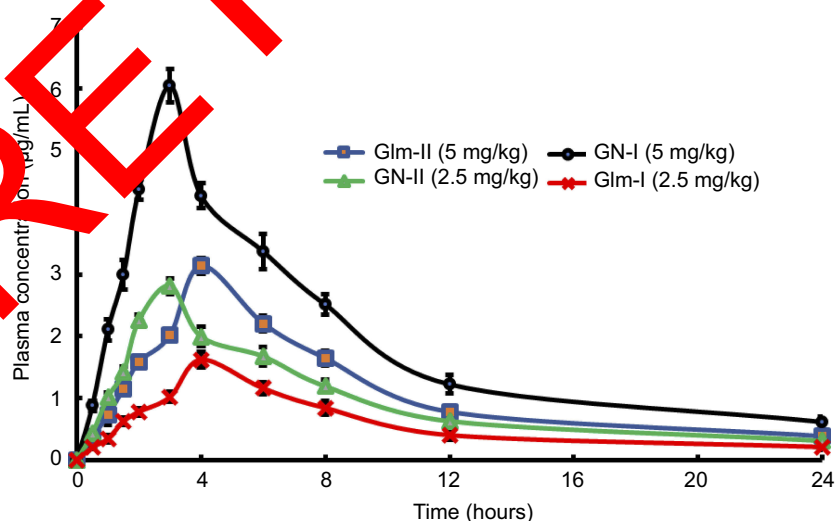


**Figure 11** Plasma drug concentration versus time after oral administration of GN and Glm.

**Abbreviations:** Glm, glimepiride; GN, Glm nanosuspension.



**Table 2** Pharmacokinetic parameters of Glm and GN

	Glm-I (5 mg/kg)	Glm-II (2.5 mg/kg)	GN-I (5 mg/kg)	GN-II (2.5 mg/kg)
<b>C<sub>max</sub> (µg/mL)</b>	3.15±0.129	1.625±0.125	6.05±0.265**	2.825±0.095**
<b>T<sub>max</sub> (hours)</b>	4±0	4±0	3±0	3±0
<b>AUC<sub>0-24</sub> (µg·h/mL)</b>	26.95±1.308	14.025±0.918	46.55±1.55***	22.8±0.392***

**Notes:** Values represent means ± SD; n=6. \*\*P<0.01, \*\*\*P<0.001 compared with unprocessed drug.

**Abbreviations:** Glm, glimepiride; GN, Glm nanosuspension; C<sub>max</sub>, maximum concentration; T<sub>max</sub>, time to C<sub>max</sub>.

**Table 3** α-Glucosidase inhibition by Glm and GN

	Concentration (µg/mL)	Percentage α-glucosidase inhibition	IC <sub>50</sub> (µg/mL)
<b>Glm</b>	1,000	77.00±0.15	49.52
	500	69.26±1.55	
	250	65.89±0.49	
	125	58.36±0.71	
	62.5	51.47±0.42	
<b>GN</b>	1,000	83.53±0.20***	21.30
	500	78.62±0.17***	
	250	73.42±0.11***	
	125	66.20±0.15**	
	62.5	61.35±0.18***	

**Notes:** Values represent means ± SD, \*\*P<0.01, \*\*\*P<0.001 compared to Glm.

**Abbreviations:** Glm, glimepiride; GN, Glm nanosuspension.

## Conclusion

Precipitation-ultrasonication was utilized for fabrication of stabilized GN. Optimized processing was found at 1% (w/v) PVP K30, 1% (w/v) HPMC, 0.12% (w/v) SLS, ultrasonication input 400 W, and 15 minutes' processing with 3-second pauses. A 300 mL batch size can be scaled up effectively utilizing this technology. The *in vitro* dissolution rate and bioavailability of Glm via the oral route were boosted distinctly by utilizing this approach for efficiently reducing the particle size to a suitable level. GN showed markedly enhanced α-glucosidase inhibition IC<sub>50</sub> compared to Glm. Glm nanosuspensions are a promising candidate for improving therapeutic activity in human volunteers. This study could play a key role in clinical evaluation of nanosuspensions in future research.

## Acknowledgments

We would like to acknowledge the Department of Pharmacy, Faculty of Life Sciences, Sarhad University of Science and Information Technology Peshawar, Khyber Pakhtunkhwa, Pakistan; the Department of Pharmacy, University of Malakand, Chakdara, Khyber Pakhtunkhwa, Pakistan; and Bryon Pharmaceuticals Pvt Limited Peshawar for their

support and provision of facilities to complete this project. The authors appreciate the Deanship of the Scientific Research at King Saud University, Saudi Arabia for funding this work through research group RG-1440-00.

## Disclosure

The authors report no conflicts of interest in this work.

## References

1. Ghosh BP, Das MK. Nanosuspension for enhancement of oral bioavailability of felodipine. *Appl Nanosci*. 2014;4(2):189–197. doi:10.1007/s13204-012-0188-3
2. Dizaj SM, Dizaj SM, Vazifehasl Z, Salatin S, Adibkia K, Javadzadeh Y. Nanosizing of drugs: effect on dissolution rate. *Res Pharm Sci*. 2015;10(2):95.
3. Sabzevari A, Adibkia K, Hashemi H, et al. Polymeric triamcinolone acetonide nanoparticles as a new alternative in the treatment of uveitis: in vitro and in vivo studies. *Eur J Pharm Biopharm*. 2013;84(1):63–71. doi:10.1016/j.ejpb.2012.12.010
4. Reverchon E. Supercritical antisolvent precipitation of micro- and nano-particles. *J Supercrit Fluids*. 1999;15(1):1–21. doi:10.1016/S0896-8446(98)00129-6
5. Pathak P, Mezziani MJ, Desai T, Sun Y-P. Formation and stabilization of ibuprofen nanoparticles in supercritical fluid processing. *J Supercrit Fluids*. 2006;37(3):279–286. doi:10.1016/j.supflu.2005.09.005
6. Li H, Wang J, Bao Y, Guo Z, Zhang M. Rapid sonocrystallization in the salting-out process. *J Cryst Growth*. 2003;247(1):192–198. doi:10.1016/S0022-0248(02)01941-3
7. Alshweiat A, Katona G, Csóka I, Ambrus R. Design and characterization of loratadine nanosuspension prepared by ultrasonic-assisted precipitation. *Eur J Pharm Sci*. 2018;122:94–104. doi:10.1016/j.ejps.2018.06.010
8. Louhi-Kultanen M, Karjalainen M, Rantanen J, Huhtanen M, Kallas J. Crystallization of glycine with ultrasound. *Int J Pharm*. 2006;320(1):23–29. doi:10.1016/j.ijpharm.2006.03.054
9. De Castro ML, Priego-Capote F. Ultrasound-assisted crystallization (sonocrystallization). *Ultrason Sonochem*. 2007;14(6):717–724. doi:10.1016/j.ultsonch.2006.12.004
10. Merisko-Liversidge EM, Liversidge GG. Drug nanoparticles: formulating poorly water-soluble compounds. *Toxicol Pathol*. 2008;36(1):43–48. doi:10.1177/0192623307310946
11. Bartos C, Ambrus R, Sipos P, et al. Study of sodium hyaluronate-based intranasal formulations containing micro- or nanosized meloxicam particles. *Int J Pharm*. 2015;491(1–2):198–207. doi:10.1016/j.ijpharm.2015.06.046
12. Jiang T, Han N, Zhao B, Xie Y, Wang S. Enhanced dissolution rate and oral bioavailability of simvastatin nanocrystal prepared by sono-precipitation. *Drug Dev Ind Pharm*. 2012;38(10):1230–1239. doi:10.3109/03639045.2011.645830

13. Zhang X, Xia Q, Gu N. Preparation of all-trans retinoic acid nanosuspensions using a modified precipitation method. *Drug Dev Ind Pharm*. 2006;32(7):857–863. doi:10.1080/03639040500534184
14. Wu TY, Guo N, Teh CY, Hay JX. *Advances in Ultrasound Technology for Environmental Remediation*. Heidelberg: Springer; 2012.
15. Bhakay A, Rahman M, Dave R, Bilgili E. Bioavailability enhancement of poorly water-soluble drugs via nanocomposites: formulation-processing aspects and challenges. *Pharmaceutics*. 2018;10(3):86. doi:10.3390/pharmaceutics10030086
16. Douroumis D, Fahr A. Nano- and micro-particulate formulations of poorly water-soluble drugs by using a novel optimized technique. *Eur J Pharm Biopharm*. 2006;63(2):173–175. doi:10.1016/j.ejpb.2006.02.004
17. Lindfors L, Forssén S, Westergren J, Olsson U. Nucleation and crystal growth in supersaturated solutions of a model drug. *J Colloid Interface Sci*. 2008;325(2):404–413. doi:10.1016/j.jcis.2008.05.034
18. Ilić I, Dreu R, Burjak M, Homar M, Kerc J, Sreć S. Microparticle size control and glimepiride microencapsulation using spray congealing technology. *Int J Pharm*. 2009;381(2):176–183. doi:10.1016/j.ijpharm.2009.05.011
19. Kumar BS, Saraswathi R, Dhanaraj SA. Solid-state characterization studies and effect of PEG 20000 and P90G on particle size reduction and stability of complexed glimepiride nanocrystals. *J Young Pharm*. 2013;5(3):83–89. doi:10.1016/j.jyp.2013.08.002
20. Tran TT-D, Tran PH-L, Nguyen MNU, et al. Amorphous isradipine nanosuspension by the sonoprecipitation method. *Int J Pharm*. 2014;474(1):146–150. doi:10.1016/j.ijpharm.2014.08.017
21. Khan S, Matas MD, Zhang J, Anwar J. Nanocrystal preparation: low-energy precipitation method revisited. *Cryst Growth Des*. 2013;13(7):2766–2777. doi:10.1021/cg4000473
22. Mohd AB, Sanka K, Bandi S, Diwan PV, Shastri N. Solid self-nanoemulsifying drug delivery system (S-SNEDDS) for oral delivery of glimepiride: development and antidiabetic activity in albino rabbits. *Drug Deliv*. 2015;22(4):499–508. doi:10.3109/10717544.2013.879777
23. Shah SMH, Ullah F, Khan S, et al. Smart nanocrystals of artemether: fabrication, characterization, and comparative in vitro and in vivo antimalarial evaluation. *Drug Des Devel Ther*. 2015;10:3837. doi:10.2147/DDDT
24. Rahim H, Sadiq A, Khan S, et al. Aceclofenac nanocrystals with enhanced in vitro, in vivo performance: formulation optimization, characterization, analgesic and acute toxicity studies. *Drug Des Devel Ther*. 2017;11:2443. doi:10.2147/DDDT
25. Du B, Shen G, Wang D, Pang L, Chen J, Liu Z. Development and characterization of glimepiride nanocrystal formulation and evaluation of its pharmacokinetic in rats. *Drug Deliv*. 2013;20(1):25–33. doi:10.3109/10717544.2012.722939
26. Mutalik S, Anju P, Manoj K, Usha A. Enhancement of dissolution rate and bioavailability of aceclofenac: a chitosan-based solvent change approach. *Int J Pharm*. 2008;350(1–2):279–290. doi:10.1016/j.ijpharm.2007.09.026
27. Artanti N, Artanti N, Tachibana S, Kardono LB, Sukiman H. Isolation of  $\alpha$ -glucosidase inhibitors produced by an endophytic fungus, *Colletotrichum sp.*, from *taxus sumatrana*. *Pak J Biol Sci*. 2012;15(1):1–3.
28. Srinta I, Srinta I, Kusumawati N, Nugerahani I, Artanti N, Xu GR. In vitro  $\alpha$ -glucosidase inhibitory activity of monascus-fermented durian seed extracts. *Int Food Res J*. 2013;20(2):533–536.
29. Merisko-Liversidge E, Liversidge GG, Cooper ER. Nanosizing: a formulation approach for poorly-water-soluble compounds. *Eur J Pharm Sci*. 2003;18(2):113–120.
30. Matteucci ME, Hotze MA, Johnston KP, Williams RO. Drug nanoparticles by antisolvent precipitation: mixing energy versus surfactant stabilization. *Langmuir*. 2006;22(21):8951–8959. doi:10.1021/la061122t
31. Lu S, Yu P-P, He J-H, et al. Enhanced dissolution and oral bioavailability of lurasidone hydrochloride nanosuspensions prepared by antisolvent precipitation-ultrasonication method. *RSC Adv*. 2016;6(54):49052–49059. doi:10.1039/C6RA08392G
32. Yadav SK, Mishra S, Mishra B. Eudragit-based nanosuspension of poorly water-soluble drug: formulation and in vitro-in vivo evaluation. *AAPS PharmSciTech*. 2012;13(4):1031–1036. doi:10.1208/s12249-012-9833-0
33. Bunjes H, Koch MH, Westesen K. Effect of particle size on colloidal solid triglycerides. *Langmuir*. 2000;16(10):5234–5241. doi:10.1021/la990856l
34. Valleri M, Mura P, Maestrelli P, Cirri M, Bordini F. Development and evaluation of glyburide fast dissolving tablets using solid dispersion technique. *Drug Dev Ind Pharm*. 2004;30(5):525–534. doi:10.1081/DDC-100037486
35. O'Mahony M, Jiang AK, Ferguson S, Cout BL, Myerson AS. A process for the formulation of nanosuspensions of active pharmaceutical ingredients with poor aqueous solubility in a nanoporous substrate. *Org Process Res Dev*. 2004;19(9):1109–1118. doi:10.1021/op500262q
36. Ali BS, Turk P, Ali AMA, Hagden N. Hydrocortisone nanosuspensions for ophthalmic delivery: a comparative study between microfluidic nanoprecipitation and wet milling. *J Controlled Release*. 2011;149(2):175–181. doi:10.1016/j.jconrel.2010.10.007
37. Wang J, Zhang J, Matanabe W. Physical and chemical stability of drug nanosuspensions. *Adv Drug Deliv Rev*. 2011;63(6):456–469. doi:10.1016/j.addr.2011.02.001
38. Fend S, Müller RH. Effect of light and temperature on zeta potential and physical stability in solid lipid nanoparticle (SLN™) dispersions. *Int J Pharm*. 1998;168(2):221–229. doi:10.1016/S0378-5173(98)00092-1
39. Jacobs C, Müller RH. Production and characterization of a budesonide nanosuspension for pulmonary administration. *Pharm Res*. 2002;19(2):189–194.
40. Prabu SL, Sharavanan S, Govindaraju S, Suriyaprakash T. Formulation development of aceclofenac nanosuspension as an alternative approach for improving drug delivery of poorly soluble drugs. *Int J Pharm Sci Nanotechnol*. 2013;6(3):2145–2153.
41. Xia D, Quan P, Piao H, et al. Preparation of stable nitrendipine nanosuspensions using the precipitation-ultrasonication method for enhancement of dissolution and oral bioavailability. *Eur J Pharm Sci*. 2010;40(4):325–334. doi:10.1016/j.ejps.2010.04.006

## International Journal of Nanomedicine

### Publish your work in this journal

The International Journal of Nanomedicine is an international, peer-reviewed journal focusing on the application of nanotechnology in diagnostics, therapeutics, and drug delivery systems throughout the biomedical field. This journal is indexed on PubMed Central, MedLine, CAS, SciSearch®, Current Contents®/Clinical Medicine,

Journal Citation Reports/Science Edition, EMBASE, Scopus and the Elsevier Bibliographic databases. The manuscript management system is completely online and includes a very quick and fair peer-review system, which is all easy to use. Visit <http://www.dovepress.com/testimonials.php> to read real quotes from published authors.

Submit your manuscript here: <https://www.dovepress.com/international-journal-of-nanomedicine-journal>